



Epitaxial growth and air-stability of monolayer Cu₂Te

K Qian(钱凯)¹, L Gao(高蕾)¹, H Li(李航)¹, S Zhang(张帅)¹, J H Yan(严佳浩)¹, C Liu(刘晨)², J O Wang(王嘉鸥)², T Qian(钱天)^{1,3}, H Ding(丁洪)^{1,3}, Y Y Zhang(张余洋)^{1,3}, X Lin(林晓)^{1,3}, S X Du(杜世萱)^{1,3}, H-J Gao(高鸿钧)^{1,3}

Citation: Chin. Phys. B . 2020, 29(1): 018104 . **doi:** 10.1088/1674-1056/ab5781

Journal homepage: <http://cpb.iphy.ac.cn>; <http://iopscience.iop.org/cpb>

What follows is a list of articles you may be interested in

Growth of high quality Sr₂IrO₄ epitaxial thin films on conductive substrates

Hui Xu(徐琿), Zhangzhang Cui(崔璋璋), Xiaofang Zhai(翟晓芳), Yalin Lu(陆亚林)

Chin. Phys. B . 2019, 28(7): 078102 . **doi:** 10.1088/1674-1056/28/7/078102

Combinatorial synthesis and high-throughput characterization of copper-oxide superconductors

J Wu, A T Bollinger, X He, I Božović

Chin. Phys. B . 2018, 27(11): 118102 . **doi:** 10.1088/1674-1056/27/11/118102

Growth of high-quality perovskite (110)-SrIrO₃ thin films using reactive molecular beam epitaxy

Kai-Li Zhang(张凯莉), Cong-Cong Fan(樊聪聪), Wan-Ling Liu(刘万领), Yu-Feng Wu(吴宇峰), Xiang-Le Lu(卢祥乐), Zheng-Tai Liu(刘正太), Ji-Shan Liu(刘吉山), Zhong-Hao Liu(刘中灏), Da-Wei Shen(沈大伟)

Chin. Phys. B . 2018, 27(8): 088103 . **doi:** 10.1088/1674-1056/27/8/088103

Effect of substrate curvature on thickness distribution of polydimethylsiloxane thin film in spin coating process

Ying Yan(闫英), Ping Zhou(周平), Shang-Xiong Zhang(张尚雄), Xiao-Guang Guo(郭晓光), Dong-Ming Guo(郭东明)

Chin. Phys. B . 2018, 27(6): 068104 . **doi:** 10.1088/1674-1056/27/6/068104

Influences of substrate temperature on microstructure and corrosion behavior of APS Ni₅₀Ti₂₅Al₂₅ inter-metallic coating

Sh Khandanjou, M Ghoranneviss, Sh Saviz, M Reza Afshar

Chin. Phys. B . 2018, 27(2): 028104 . **doi:** 10.1088/1674-1056/27/2/028104

RAPID COMMUNICATION

Epitaxial growth and air-stability of monolayer Cu₂Te*

K Qian(钱凯)¹, L Gao(高蕾)¹, H Li(李航)¹, S Zhang(张帅)¹, J H Yan(严佳浩)¹, C Liu(刘晨)²,
J O Wang(王嘉鸥)², T Qian(钱天)^{1,3}, H Ding(丁洪)^{1,3}, Y Y Zhang(张余洋)^{1,3},
X Lin(林晓)^{1,3,‡}, S X Du(杜世萱)^{1,3,†}, and H-J Gao(高鸿钧)^{1,3}

¹Institute of Physics & University of Chinese Academy of Sciences, Chinese Academy of Sciences, Beijing 100190, China

²Institute of High Energy Physics, Chinese Academy of Sciences, Beijing 100049, China

³CAS Center for Excellence in Topological Quantum Computation, University of Chinese Academy of Sciences, Beijing 100190, China

(Received 1 November 2019; revised manuscript received 8 November 2019; accepted manuscript online 14 November 2019)

A new two-dimensional atomic crystal, monolayer cuprous telluride (Cu₂Te) has been fabricated on a graphene-SiC(0001) substrate by molecular beam epitaxy (MBE). The low-energy electron diffraction (LEED) characterization shows that the monolayer Cu₂Te forms a $\sqrt{3} \times \sqrt{3}$ superstructure with respect to the graphene substrate. The atomic structure of the monolayer Cu₂Te is investigated through a combination of scanning tunneling microscopy (STM) experiments and density functional theory (DFT) calculations. The stoichiometry of the Cu₂Te sample is verified by x-ray photoelectron spectroscopy (XPS) measurement. The angle-resolved photoemission spectroscopy (ARPES) data present the electronic band structure of the sample, which is in good agreement with the calculated results. Furthermore, air-exposure experiments reveal the chemical stability of the monolayer Cu₂Te. The fabrication of this new 2D material with a particular structure may bring new physical properties for future applications.

Keywords: cuprous telluride (Cu₂Te), scanning tunneling microscopy (STM), density functional theory (DFT), chemical stability

PACS: 81.15.-z, 81.05.Zx, 81.07.Bc

DOI: 10.1088/1674-1056/ab5781

1. Introduction

Since the discovery of graphene,^[1] the research of two-dimensional (2D) atomic crystal materials has developed rapidly.^[2–4] Transition metal chalcogenides (TMCs) have received much attention because of their diversity and unique properties.^[5,6] For example, the non-magnetic silver chalcogenide has been reported for its large magnetoresistance^[7] and Ag₂Te has been theoretically identified as a new topological insulator.^[8] Additionally, TMDCs are well known for their novel optical and electronic properties as well as strong spin-orbit coupling effects.^[5,9] TMDCs, such as MoS₂, have indirect to direct bandgap arising from their strict dimensional confinement, allowing for applications such as photodetectors and transistors.^[10–12]

Cu₂Te, an important member of the TMCs, has attracted significant attention due to its recent developments in thermoelectric and optoelectronics.^[13–17] Cu₂Te is also commonly used to form back contacts to improve the performance of thin-film solar cell.^[18–20] However, the structural determination of Cu₂Te remains controversial. Although several structures have been proposed experimentally and theoretically,^[16,21–23] the atomic position in the structure remains unsolved. The hexag-

onal phase, proposed 70 years ago,^[22] has been theoretically proved energetically unfavorable.^[23]

In this paper, we report the fabrication of high-quality monolayer Cu₂Te on bilayer graphene (BLG)/SiC(0001) by molecular beam epitaxy (MBE) method and the characterization of its structure at atomic level. The stoichiometry and the atomic structure of the monolayer Cu₂Te are determined by x-ray photoelectron spectroscopy (XPS), scanning tunneling microscopy (STM), low energy electron diffraction (LEED) experiments and density functional theory (DFT) calculation. We reveal that the monolayer Cu₂Te crystallizes in a hexagonal structure with the space group *P*-3m1. Angle-resolved photoemission spectroscopy (ARPES) is used to study the electronic band structure of the monolayer Cu₂Te, and the result is in good agreement with the DFT calculated band structure. Moreover, our experiment shows that the Cu₂Te monolayer is quite inert in air. The monolayer Cu₂Te with good chemical stability serves as a promising candidate for 2D electronics.

2. Methods

Sample preparation and characterizations The sam-

*Project supported by the National Key Research & Development Program of China (Grant Nos. 2016YFA0202300 and 2018YF A0305800), the National Natural Science Foundation of China (Grant Nos. 61888102, 11604373, 61622116, and 51872284), the CAS Pioneer Hundred Talents Program, China, the Strategic Priority Research Program of Chinese Academy of Sciences (Grant Nos. XDB30000000 and XDB28000000), Beijing Nova Program, China (Grant No. Z181100006218023), and the University of Chinese Academy of Sciences. A portion of the research was performed in the CAS Key Laboratory of Vacuum Physics. Computational resources were provided by the National Supercomputing Center in Tianjin.

†Corresponding author. E-mail: sxdu@iphy.ac.cn

‡Corresponding author. E-mail: mlin@ucas.ac.cn

ple was fabricated in a commercial UHV system (Omicron) with standard molecular beam epitaxy (MBE) chamber. The large-scale uniform bilayer graphene on 6H-SiC(0001) wafer was formed by flashing the wafer to 1550 K in ultrahigh vacuum.^[24] The quality of the bilayer graphene was verified by LEED and STM. The monolayer Cu₂Te sample was fabricated on the bilayer graphene by co-deposition of copper and tellurium atoms from an e-beam evaporator and a standard Knudsen diffusion cell, respectively, while the SiC substrate was held at 400 K during the growth process. The STM, ARPES, LEED, and XPS characterizations were performed at room temperature. ARPES measurements were performed by using the He II ($h\nu = 40.6$ eV) resonance lines and a VG SCI-ENTA R4000 analyzer. The angular and energy resolutions were set to 0.2° and 30 meV, respectively. The experiments were carried out with a commercial high-resolution LEED instrument (OCI). Typical emission currents were in the range of 1–5 nA and beam energies were between 0 eV and 120 eV. The XPS experiments were carried out at the Beijing Synchrotron Radiation Facility. The photon energy ranges from 10 eV to 1100 eV. There were four high resolution gratings for realizing the monochromatic synchrotron radiation light.

First-principles calculations Quantum mechanical calculations based on density functional theory (DFT) were performed using the Vienna *ab initio* simulation package (VASP).^[25,26] The projector augmented wave (PAW) method

and the local-density approximation (LDA)^[27,28] for the exchange–correlation functional were adopted. The rotationally invariant LDA + *U* formalism proposed by Dudarev *et al.*^[29] was used with $U_{\text{eff}} = 6.52$ eV for Cu.^[30] 450 eV energy cutoff and 15 Å vacuum layers were used for structure relaxations. The total energies were converged to 10^{-4} eV, and forces were converged to 0.001 eV/Å. The *k*-points sampling was $39 \times 39 \times 1$.

3. Results and discussion

Figure 1(a) shows a typical large scale STM image of the as-grown sample. Cu₂Te forms a flat island on bilayer graphene substrate, and the apparent height of the island is ~ 0.85 nm (Fig. 1(b)), which is measured by the STM line profile crossing the edge of the island (corresponding to the blue line in Fig. 1(a)). The symmetry of Cu₂Te on BLG is characterized by LEED. As previously reported,^[31] some of the LEED spots originate from the BLG/SiC(0001) substrate. The red, white, and sky-blue arrows point to the spots from BLG, SiC, and moiré pattern, respectively (Fig. 1(c)). After the growth of Cu₂Te, six new diffraction spots appear at the $(\sqrt{3} \times \sqrt{3})$ positions with respect to the graphene spots as indicated by the yellow dashed circles. The LEED pattern of Cu₂Te on BLG/SiC(0001) suggests that the formed Cu₂Te island on bilayer graphene is well-ordered.

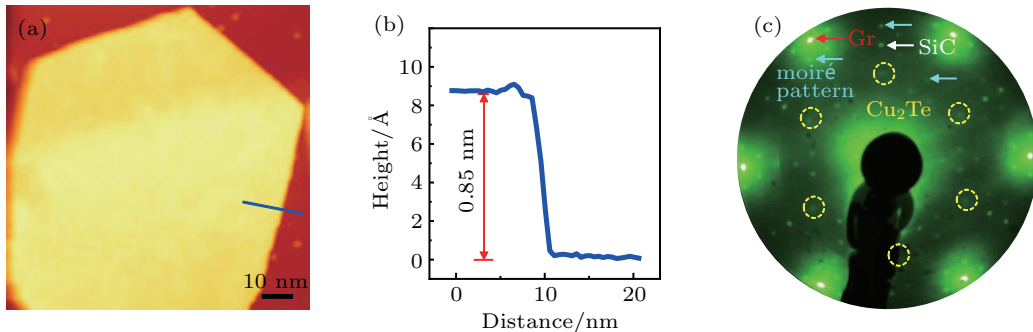


Fig. 1. Cu₂Te island grown on bilayer graphene. (a) An STM topographic image (−1 V, −10 pA) of the Cu₂Te island on bilayer graphene. (b) The line profile along the blue line in (a) shows that the apparent height of the Cu₂Te island is ~ 0.85 nm. (c) LEED pattern of Cu₂Te grown on bilayer graphene on SiC(0001). The diffraction spots of graphene, SiC, and moiré pattern are indicated by red, white, and sky-blue arrows, respectively. LEED spots indicated by yellow circles originate from Cu₂Te, and present a $(\sqrt{3} \times \sqrt{3})$ structure with respect to the graphene substrate.

In order to further investigate the sample in detail, high resolution STM and XPS characterizations were performed. The atomic resolution STM image (Fig. 2(a)) of Cu₂Te shows hexagonally arranged protrusions with a lattice constant of ~ 0.41 nm (Fig. 2(b)). Figures 2(c) and 2(d) are the characteristic XPS spectra from the core levels of Te and Cu, respectively. As shown in Fig. 2(c), the peaks at 583.1 eV and 572.8 eV are assigned to Te 3d_{3/2} and Te 3d_{5/2}, respectively. In Fig. 2(d), the Cu 2p core level spectrum has two peaks at 952.6 eV (Cu 2p_{1/2}) and 932.8 eV (Cu 2p_{3/2}). All of these XPS results are in good agreement with previous report for nanoflake Cu₂Te.^[14] It should be emphasized that there is no

satellite peaks and all the peaks are sharp, supporting the formation of pure Cu₂Te.

Based on these experimental results and previous prediction of bulk layered Cu₂Te,^[21] we propose an atomic model of the monolayer Cu₂Te, as shown in Fig. 2(e). It contains six atomic layers and the terminated layers are only made of selenium atoms while four copper layers are in the middle. The DFT-calculated relaxed lattice constants are 0.40 nm, which is in agreement with the experimental value of 0.41 nm. Based on this monolayer Cu₂Te structure model, we simulate an STM image (Fig. 2(f)), which presents all the features in experimental STM image very well. We unveil the configura-

tion of monolayer Cu_2Te at atomic scale for the first time.

The electronic band structure of the monolayer Cu_2Te is investigated by *in situ* ARPES measurement combining with first-principle calculations. Figure 3(a) is the ARPES result of the monolayer Cu_2Te . Along the Γ - K direction, the band structure shows a significant feature that there are two degenerate bands around the Fermi surface. To obtain more details of the band structure of the monolayer Cu_2Te , the energy bands are calculated based on the monolayer Cu_2Te structure model, and presented in Fig. 3(b). It can be seen that the agreement between the ARPES experimental data and the calculated energy bands is quite good. There are four bands around the Fermi level, but they are too close to be distinguished by the ARPES experiment. For the first time, the band structure of the monolayer Cu_2Te has been determined experimentally.

Furthermore, the chemical stability, especially the air stability, is critical for low dimensional materials in practical

applications, such as photodetectors and nano-electronic devices. The air-exposure experiment of the monolayer Cu_2Te on BLG/SiC(0001) sample was performed. The sample was taken out of the ultra-high vacuum chamber and exposed to air for half an hour. Then, the sample was transferred back into the ultra-high vacuum chamber and mildly annealed at 400 K to remove the possible physisorbed species. Finally, the monolayer Cu_2Te was characterized by STM. As shown in Fig. 4(a), the topographic STM image reveals that the Cu_2Te island is intact and the island surface is clean and smooth. Figure 4(b) is an atomic resolution STM image of the sample which has been exposed to the air. It is clear that there are no defects and the hexagonal structure remains the same. The air-exposure experiment reveals the chemical robustness of the monolayer Cu_2Te , and this chemical inertness makes the monolayer Cu_2Te have potential for future applications.

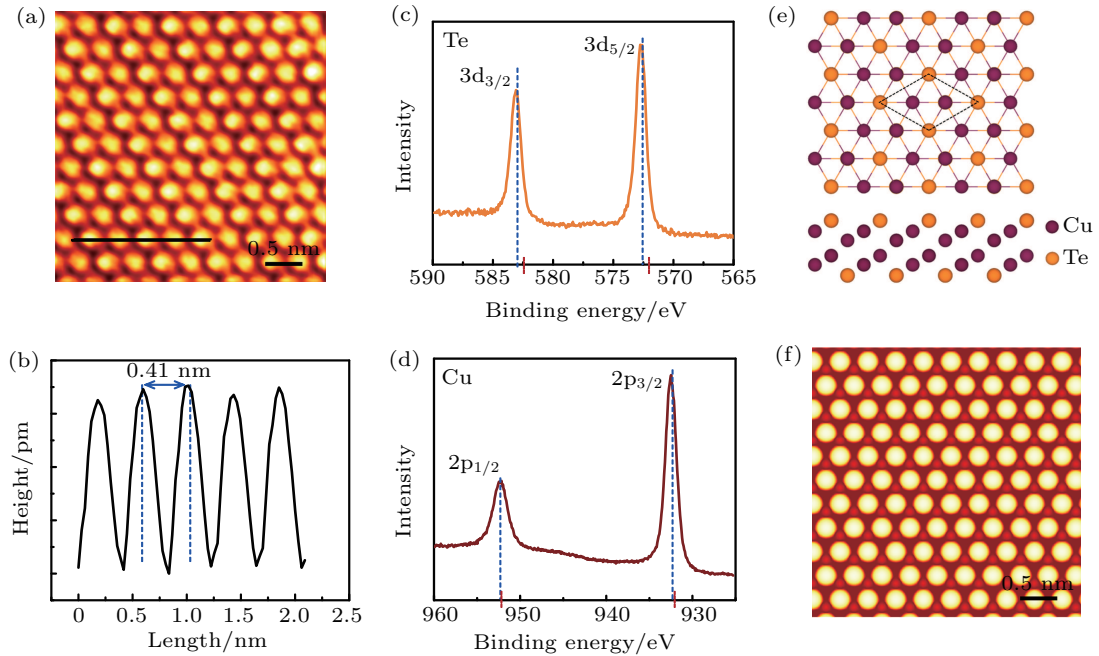


Fig. 2. Atomic configuration and the XPS results of the monolayer Cu_2Te . (a) An atomic resolution STM image of monolayer Cu_2Te . (b) Line profile of the Cu_2Te sample corresponding to the black line in (a). The periodicity of the monolayer Cu_2Te lattice is ~ 0.41 nm. (c) The XPS core-level spectrum of Te. The peak positions are 583.1 eV ($3d_{3/2}$) and 572.8 eV ($3d_{5/2}$). (d) The Cu 2p XPS spectrum. The peak positions are 952.6 eV ($2p_{1/2}$) and 932.8 eV ($2p_{3/2}$). (e) The atomic model of the monolayer Cu_2Te . The dotted rhombus indicates the unit cell of the Cu_2Te monolayer. (f) Simulated STM image of the monolayer Cu_2Te .

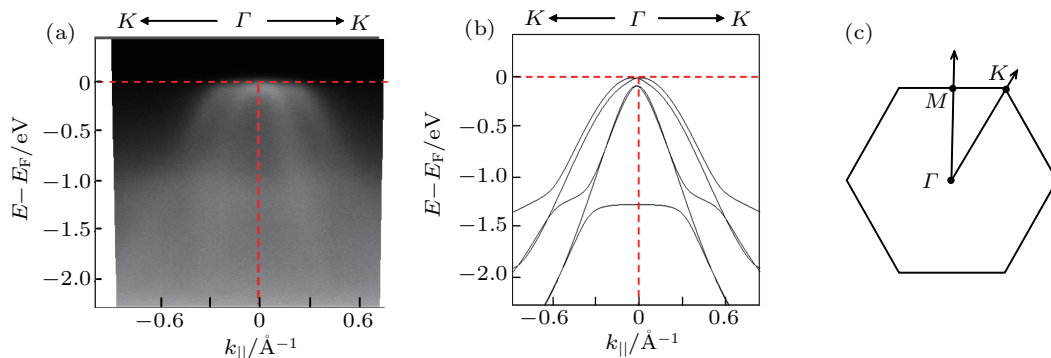


Fig. 3. ARPES experimental results and DFT calculated results of the electronic structure of the monolayer Cu_2Te . (a) The electronic band structure measured by ARPES along the Γ - K direction. (b) The DFT calculated band structure along the Γ - K direction. (c) Brillouin zone of the monolayer Cu_2Te .

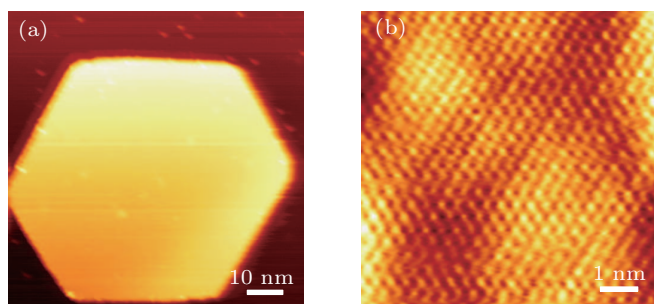


Fig. 4. Air stability of the monolayer Cu_2Te . (a) An STM image of a Cu_2Te island on bilayer graphene after exposing to air for 30 min ($V_s = -1$ V, $I_t = 0.1$ nA). (b) The high resolution STM image of the Cu_2Te surface after exposing to air ($V_s = -0.5$ V, $I_t = 0.5$ nA).

4. Conclusion

We have successfully fabricated monolayer Cu_2Te on bilayer graphene/SiC(0001) substrate by the MBE method. The *in situ* STM, LEED, and XPS measurements verify the quality of the monolayer Cu_2Te . An atomic structure model of the monolayer Cu_2Te is proposed and DFT calculations confirm the model. Moreover, the ARPES results are in good agreement with the calculated energy bands, which further confirms the structure of the monolayer Cu_2Te . Finally, air exposure experiments demonstrate the air stability of the monolayer Cu_2Te . Our work provides a new 2D material, Cu_2Te , and it has the potential for applications in the future nano-devices.

References

- [1] Novoselov K S, Geim A K, Morozov S V, Jiang D, Zhang Y, Dubonos S V, Grigorieva I V and Firsov A A 2004 *Science* **306** 666
- [2] Mounet N, Gibertini M, Schwaller P, Campi D, Merkys A, Marrazzo A, Sohier T, Castelli I E, Cepellotti A, Pizzi G and Marzari N 2018 *Nat. Nanotech.* **13** 246
- [3] Geim A K and Grigorieva I V 2013 *Nature* **499** 419
- [4] Hao Y, Wang L, Liu Y, Chen H, Wang X, Tan C, Nie S, Suk J W, Jiang T, Liang T, Xiao J, Ye W, Dean C R, Yakobson B I, McCarty K F, Kim P, Hone J, Colombo L and Ruoff R S 2016 *Nat. Nanotech.* **11** 426
- [5] Wang Q H, Kalantar-Zadeh K, Kis A, Coleman J N and Strano M S 2012 *Nat. Nanotech.* **7** 699
- [6] Yang H, Kim S W, Chhowalla M and Lee Y H 2017 *Nat. Phys.* **13** 931
- [7] R Xu A H, Rosenbaum T F, Saboungi M L and Littlewood P B 1997 *Nature* **390** 57
- [8] Zhang W, Yu R, Feng W X, Yao Y G, Weng H M, Dai X and Fang Z 2011 *Phys. Rev. Lett.* **106** 156808
- [9] Schaibley J R, Yu H, Clark G, Rivera P, Ross J S, Seyler K L, Yao W and Xu X 2016 *Nat. Rev. Mater.* **1** 16055
- [10] Splendiani A, Sun L, Zhang Y B, Li T S, Kim J, Chim C Y, Galli G and Wang F 2010 *Nano Lett.* **10** 1271
- [11] Mak K F, He K L, Shan J and Heinz T F 2012 *Nat. Nanotech.* **7** 494
- [12] Rivera P, Seyler K L, Yu H Y, Schaibley J R, Yan J Q, Mandrus D G, Yao W and Xu X D 2016 *Science* **351** 688
- [13] Park D, Ju H, Oh T and Kim J 2018 *Sci. Rep.* **8** 18082
- [14] Cheng L, Wang M, Pei C, Liu B, Zhao H, Zhao H, Zhang C, Yang H and Liu S 2016 *RSC. Adv.* **6** 79612
- [15] Ballikaya S, Chi H, Salvador J R and Uher C 2013 *J. Mate. Chem. A* **1** 12478
- [16] Zhang Y, Wang Y, Xi L, Qiu R, Shi X, Zhang P and Zhang W 2014 *J. Chem. Phys.* **140** 074702
- [17] Han C, Bai Y, Sun Q, Zhang S, Li Z, Wang L and Dou S 2016 *Adv. Sci. (Weinh)* **3** 1500350
- [18] Yun J H, Kim K H, Lee D Y and Ahn B T 2003 *Sol. Energy. Mat. Sol. C* **75** 203
- [19] Woodbury H H and Aven M 1968 *J. Appl. Phys.* **39** 5485
- [20] Lv B, Di X, Li W, Feng L H, Lei Z, Zhang J Q, Wu L L, Cai Y P, Li B and Sun Z 2009 *Jpn. J. Appl. Phys.* **48** 085501
- [21] Nguyen M C, Choi J H, Zhao X, Wang C Z, Zhang Z and Ho K M 2013 *Phys. Rev. Lett.* **111** 165502
- [22] Nowotny Z M 1946 *Phys. Rep.* **37** 40
- [23] Da Silva J L F, Wei S H, Zhou J and Wu X Z 2007 *Appl. Phys. Lett.* **91** 091902
- [24] Wang Q, Zhang W, Wang L, He K, Ma X and Xue Q 2013 *J. Phys: Condens. Matter* **25** 095002
- [25] Kresse G and Furthmüller J 1996 *Phys. Rev. B* **54** 11169
- [26] Kresse G and Furthmüller J 1996 *Comput. Mater. Sci.* **6** 15
- [27] Ceperley D M and Alder B J 1980 *Phys. Rev. Lett.* **45** 566
- [28] Perdew J P and Zunger A 1981 *Phys. Rev. B* **23** 5048
- [29] Dudarev S L, Botton G A, Savrasov S Y, Humphreys C J and Sutton A P 1998 *Phys. Rev. B* **57** 1505
- [30] Wu D, Zhang Q and Tao M 2006 *Phys. Rev. B* **73** 235206
- [31] Riedl C, Coletti C, Iwasaki T, Zakharov A A and Starke U 2009 *Phys. Rev. Lett.* **103** 246804